

A METHOD TO DETERMINE ALLOWABLE SPEED FOR A UNIT LOAD IN A PALLET FLOW RACK

Eugene SAFRONOV,* Andrey NOSKO*

*Bauman Moscow State Technical University, Faculty of Robotics and Complex Automation, Department of Lifting and Transport Systems,
105005, Moscow, 2-ya Baumanskaya 5/1, Russian Federation

gen-s@mail.ru, dr.nosko@mail.ru

received 4 January 2019, revised 26 April 2019, accepted 30 April 2019

Abstract: Pallet flow rack are widely used in intralogistics to maximize warehouse capacity and to reduce the travel by fork-lifts. However, the use of pallet flow racks is associated with increased danger due to the use of gravity conveyors in their design. For this purpose, the gravity conveyors of pallet flow rack have a two safety elements – brake rollers and a stopping mechanism with pallet separator, which are working as a system. Brake rollers limit the speed of pallets, while the stopping mechanism allows exerting a pressure on the unloading pallet from the following behind it. A pallet should have such a speed, controlled by the brake rollers, so that it could be stopped by a stopping mechanism without damaging it. Based on the Cox impact theory, an original method for determining the allowable speed of a pallet in a pallet flow rack is proposed. The method ensures safe operation of the stopping mechanism with pallet separator and takes into account the mechanical properties and design parameters of the pallet separator stopper. A calculation example is provided for the most commonly used types of pallets – Euro pallet (1200 mm × 800 mm) and Industrial pallet (1200 mm × 1000 mm). The obtained results agree well with the pallet speed range of 0.2 to 0.3 m/s recommended by the manufacturers of pallet flow racks.

Key words: Gravity roller conveyor, pallet flow rack, dynamic pallet rack, pallet speed

1. INTRODUCTION

Reducing the cost of warehouse operations is one of the main tasks in the designing of warehouses and the selection of material handling equipment and storage systems. Solutions of this task can be found by optimizing space utilization (e.g., Derhami et al., 2017), reducing the total travelled distance by the fork-lifts (Ghalekhondabi and Masel, 2018), using automated storage and retrieval systems (AS/RSs), autonomous vehicle storage and retrieval systems (AVS/RSs) (Heragu et al., 2011) and Shuttle-Based Storage and Retrieval Systems (SBS/Rs) (Lerher et al., 2017) for increasing the throughput of warehouse operations.

Optimizing space utilization of a warehouse and maximising warehouse capacity, also reducing the travel by fork-lifts, can be achieved with block storage or deep-lane storage systems (Sulirova et al., 2017; Boysen et al., 2018; Boywitz and Boysen, 2018). One of such systems is pallet flow rack (Fig. 1) (Accorsi et al., 2017 and Eo et al., 2015).

The construction of a pallet flow rack can be divided into two parts – static and dynamic. The static part includes standard racking elements, which provide stability in each direction as well as support for dynamic elements. The dynamic part includes a gravity roller conveyor and safety elements, such as brake rollers and a stopping mechanism with pallet separator (Vujanac et al., 2016) (Fig. 2). Pallets are the most common form of unit loads in warehouses. There are various types of pallets, of which Euro pallet (1200 mm × 800 mm) and Industrial pallet (1200 mm × 1000 mm) are widely used in the EU as well as in other countries (Rushton et al., 2010). The maximum pallet weight during trans-

portation is determined experimentally for each type of product. The safe operation load is limited to 1250 kg (EPAL Euro Pallet).

As noted by Wu S et al. (2016), pallet flow racks save 22–25% of travelled distance by fork-lifts in comparison with single-deep racks. Therefore, pallet flow racks are widely using in automated warehouses with AS/RSs machines (Metahri and Hachemi, 2017; Ghomri and Sari, 2017; Hamzaoui and Sari, 2015), automated compact cross-dock system (Zaerpour et al., 2015) and with Just-In-Time production system (Halim et al., 2012).

However, the use of pallet flow racks is associated with increased danger due to the use of gravity conveyors in their design. At the same time, studies of the static part are widely reflected in the literature (e.g., Thombare et al., 2016; Talebian et al., 2018; Crisan et al., 2012; Saleh et al., 2018), in contrast to the safety elements of pallet flow racks – brake rollers and a stopping mechanism with pallet separator (Vujanac et al., 2016).

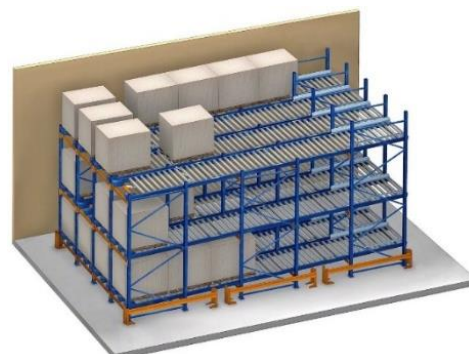


Fig. 1. Pallet flow rack

As is known, human factor is one of the main causes of accidents on a production (Aleksandrov et al., 2016), and utilization of stopping mechanism with pallet separator allows to reduce the requirements for the fork-lift drivers working with pallet flow racks due to the exclusion of pressure on the unloading pallet from the following behind it.

A pallet should have such a speed so that it could be stopped by a stopping mechanism without damaging it. This condition is achieved by the utilization of brake rollers (Nosko et al, 2018).

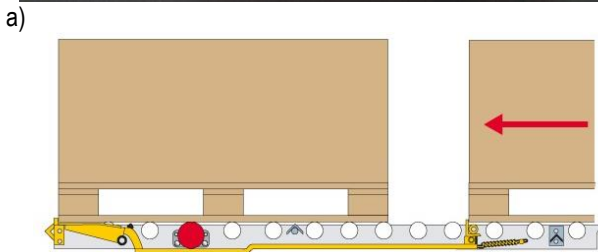


Fig. 2. Safety elements of a pallet flow rack: a) brake roller; b) stopping mechanism with pallet separator

In addition, in gravity roller conveyors as well as in pallet flow racks using such conveyors, it is usually required to limit the speed of unit loads (Kulwiec, 1985). This requirement is pointed in some national standards of safety, for example, POT R M-029-2003 in Russia.

In practice, manufacturers recommend safe transportation speed to be in the range of 0.2 to 0.3 m/s. However, it was not possible to find methods for determining this speed.

The purpose of this study is to develop a method for calculating the allowable speed for pallets of different masses in a gravity rack.

2. ALLOWABLE LOAD ON THE STOPPER

When the pallet is transported by the gravity roller conveyor, it hits the stopper of stopping mechanism with pallet separator (hereinafter the 'stopper') from the side of the discharge.

In more than 90% of cases, a pallet is oriented along the gravity roller conveyor. Thereby, the impact of the pallet sump against a stopper occurs at the three lug faces, as shown in Fig. 3.

Review of patent and bibliographic sources including catalogues of such companies like Interroll, Damon Group, Rack & Roll, Mecalux and Euroroll showed that the most often used construction of the stopper represents a square or round cross-section tube with a welded plate. Such a stopper is schematically shown in Fig. 4.

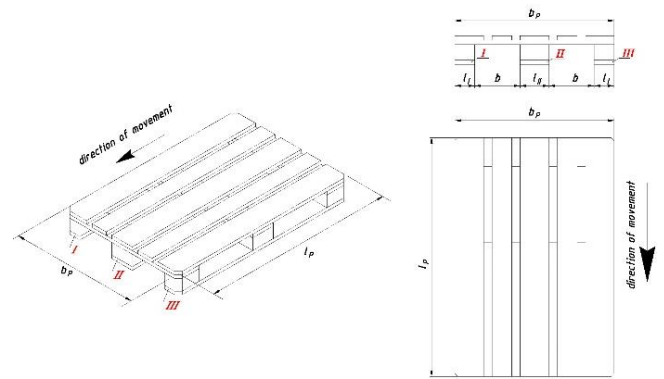


Fig. 3. Parameters of a pallet

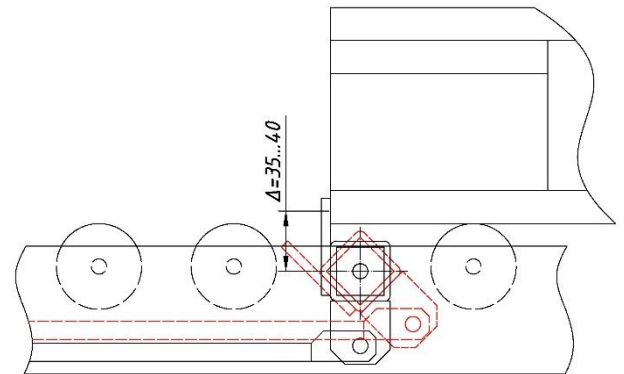


Fig. 4. Cross-section of the stopper

In the process of stopping the pallet, an off-centre impact occurs, resulting in bending and torsional deformations of the stopper. The schematic of the loading and the distributions of the bending moment and torque in the stopper is shown in Fig. 5. Because of the symmetry, a half of the stopper can be considered, for example, the sections 1-4. The geometric parameters of the stopper are presented in Table 1.

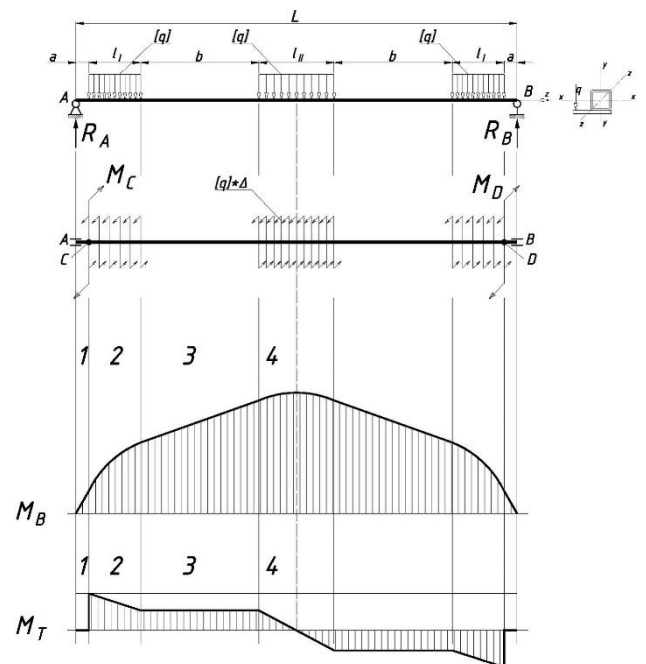


Fig. 5. Distributions of the bending moment and torque in the stopper

Tab. 1. Geometric parameters of the stopper

Type of pallet	L, mm	a, mm	l _i , mm	b, mm	l _{II} , mm	Δ, mm
Euro pallet	880	40	100	227.5	145	35–40
Industrial pallet	1100	50	145	282.5	145	

According to Fig. 5, the bending moment M_{iB} for the i -th section of the stopper can be calculated as follows:

$$\left\{ \begin{array}{l} M_{1B}(z) = R_A \cdot z = q \left(l_i + \frac{l_{II}}{2} \right) z, 0 \leq z \leq a \\ M_{2B}(z) = \left(l_i + \frac{l_{II}}{2} - \frac{z}{2} \right) qz + M_{1B}^{z=a}, 0 \leq z \leq l_i \\ M_{1B}^{z=a} = q \left(l_i + \frac{l_{II}}{2} \right) a \\ M_{3B}(z) = \frac{l_{II}}{2} qz + M_{2B}^{z=l_i}, 0 \leq z \leq b \\ M_{2B}^{z=l_i} = \left(\frac{l_{II}}{2} + \frac{l_i}{2} \right) ql_i + q \left(l_i + \frac{l_{II}}{2} \right) \cdot a \\ M_{4B}(z) = (l_{II} - z) \frac{qz}{2} + M_{3B}^{z=b}, 0 \leq z \leq \frac{l_{II}}{2} \\ M_{3B}^{z=b} = \frac{l_{II}}{2} qb + \left(\frac{l_{II}}{2} + \frac{l_i}{2} \right) ql_i + q \left(l_i + \frac{l_{II}}{2} \right) \cdot a \\ M_{B_MAX} = M_{4B}^{z=l_{II}/2} = \frac{ql_{II}^2}{4} + M_{3B}^{z=b} \end{array} \right. \quad (1)$$

where: M_{iB} is the bending moment for the i -th section; z is the axial coordinate; M_{B_MAX} is the maximum bending moment; q is the distributed load.

We represent the bending moments in matrix form as:

$$\begin{pmatrix} M_{1B}(z) \\ M_{2B}(z) \\ M_{3B}(z) \\ M_{4B}(z) \end{pmatrix} = q \cdot \begin{pmatrix} A_{1B} & B_{1B} & C_{1B} \\ A_{2B} & B_{2B} & C_{2B} \\ A_{3B} & B_{3B} & C_{3B} \\ A_{4B} & B_{4B} & C_{4B} \end{pmatrix} \cdot \begin{pmatrix} z^2 \\ z \\ 1 \end{pmatrix} \quad (2)$$

where: A_{iB} , B_{iB} , C_{iB} are constant coefficients. Taking account of Eq. (1) and Eq. (2), these coefficients are calculated as:

$$\begin{pmatrix} A_{1B} & B_{1B} & C_{1B} \\ A_{2B} & B_{2B} & C_{2B} \\ A_{3B} & B_{3B} & C_{3B} \\ A_{4B} & B_{4B} & C_{4B} \end{pmatrix} = \begin{pmatrix} 0 & l_i + 0.5l_{II} & 0 \\ -0.5 & l_i + 0.5l_{II} & \left(l_i + \frac{l_{II}}{2} \right) a \\ 0 & 0.5l_{II} & (l_i + 0.5l_{II})(l_i + a) - 0.5l_i^2 \\ -0.5 & 0.5l_{II} & (l_i + 0.5l_{II})(l_i + a) - 0.5l_i^2 + 0.5bl_{II} \end{pmatrix} \quad (3)$$

According to Fig. 5, the torque M_{iT} for the i -th section of the stopper can be calculated as follows:

$$\left\{ \begin{array}{l} M_{1T}(z) = 0, 0 \leq z \leq a \\ M_{2T}(z) = \left(l_i + \frac{l_{II}}{2} - z \right) \cdot q \cdot \Delta, 0 \leq z \leq l_i \\ M_{3T}(z) = M_{2T}^{z=l_i}, 0 \leq z \leq b \\ M_{2T}^{z=l_i} = \frac{l_{II}}{2} \cdot q \cdot \Delta \\ M_{4T}(z) = M_{3T}^{z=b} - z \cdot q \cdot \Delta, 0 \leq z \leq \frac{l_{II}}{2} \\ M_{3T}^{z=b} = \frac{l_{II}}{2} \cdot q \cdot \Delta, \end{array} \right. \quad (4)$$

where: M_{iT} is the torque for the i -th section; z is the axial coordi-

nate; M_{B_MAX} is the maximum bending moment; q is the distributed load, Δ is the moment arm (see Fig. 5 and Table 1).

We represent the torque in matrix form as:

$$\begin{pmatrix} M_{1T}(z) \\ M_{2T}(z) \\ M_{3T}(z) \\ M_{4T}(z) \end{pmatrix} = q\Delta \begin{pmatrix} B_{1T} & C_{1T} \\ B_{2T} & C_{2T} \\ B_{3T} & C_{3T} \\ B_{4T} & C_{4T} \end{pmatrix} \begin{pmatrix} z \\ 1 \end{pmatrix} \quad (5)$$

where: B_{iT} , C_{iT} are constant coefficients. Taking account of Eq. (4) and Eq. (5), these coefficients are calculated as:

$$\begin{pmatrix} B_{1T} & C_{1T} \\ B_{2T} & C_{2T} \\ B_{3T} & C_{3T} \\ B_{4T} & C_{4T} \end{pmatrix} = \begin{pmatrix} 0 & 0 \\ -1 & l_i + l_{II}/2 \\ 0 & l_{II}/2 \\ -1 & l_{II}/2 \end{pmatrix} \quad (6)$$

According to Fig. 5, dangerous section of the stopper is third section with $z = b$ or:

$$\left\{ \begin{array}{l} M_{3B}^{z=b} = \frac{l_{II}}{2} qb + \left(\frac{l_{II}}{2} + \frac{l_i}{2} \right) ql_i + q \left(l_i + \frac{l_{II}}{2} \right) \cdot a \\ M_{3T}^{z=b} = \frac{l_{II}}{2} \cdot q \cdot \Delta \end{array} \right. \quad (7)$$

We represent bending moment and torque in the dangerous section of the stopper as:

$$\left\{ \begin{array}{l} M_B = M_{3B}^{z=b} = K_B \cdot q \\ M_T = M_{3T}^{z=b} = K_T \cdot q' \end{array} \right. \quad (8)$$

where: K_B – coefficient of bending moment, K_T – torque coefficient.

The coefficients K_B and K_T are calculated with account of the data of Tab. 1.

Tab. 2 presents the values of K_B , M_B , K_T and M_T obtained using Eq. (7) and Eq. (8) for different pallet sizes.

Tab. 2. The values of coefficients K_B and K_T and expressions for calculating the maximum values of the bending moment and torque

Type of pallet	K_B , m ²	M_B , Nm	K_T , m ²	M_T , Nm
Euro pallet	0.0356	0.0356 q	0.0029	0.0029 q
Industrial pallet	0.035	0.035 q	0.002	0.002 q

Concerning the Mises yield criterion, the maximum allowable stress of the stopper is calculated (Jones R., 2009) as follows:

$$[\sigma] = \sqrt{\left(\frac{M_B \cdot Y_{MAX}}{I_X} \right)^2 + 3 \left(\frac{M_T \cdot R_{MAX}}{I_T} \right)^2} \quad (9)$$

where: I_X – the second moment of area about the neutral axis X , Y_{MAX} – the maximum perpendicular distance to the neutral axis X , I_T – torsional constant of the cross-sectional shape of the stopper, R_{MAX} – the maximum distance from the axis of torsion to the point of section with maximum torsional stress.

Taking into account Eq. (8) and Eq. (9), the allowable distributed load $[q]$ is calculated as below:

$$[q] = \frac{[\sigma]}{\sqrt{\left(\frac{K_B \cdot Y_{MAX}}{I_X}\right)^2 + 3\left(\frac{K_T \cdot R_{MAX}}{I_T}\right)^2}} \quad (10)$$

3. STRAIN ENERGY OF THE STOPPER

According to Fig. 5, the strain energy of the stopper is determined by the sum of independent works of the two factors: bending moment and torque, and calculated as (Nash, 1998):

$$U = \frac{1}{2} \int_l \left(\frac{M_T^2}{G \cdot I_T} + \frac{M_B^2}{E \cdot I_X} \right) dz \quad (11)$$

where: G – modulus of elasticity in shear, E – the Young’s modulus.

Taking into account Eq. (1), Eq. (2) and Eq. (11), and because of the symmetry, strain energy from work of bending moment for i -th section is found using the formula:

$$(U_B)_i = \frac{1}{2} \int_l \frac{2 \cdot M_{iB}^2}{E \cdot I_X} dz = q^2 \cdot \int_l \frac{(A_{iB} \cdot z^2 + B_{iB} \cdot z + C_{iB})^2}{E \cdot I_X} dz$$

Or in more convenient form as:

$$(U_B)_i = \frac{q^2}{E \cdot I_X} \cdot (K_{1iB} \cdot z_i + K_{2iB} \cdot z_i^2 + K_{3iB} \cdot z_i^3 + K_{4iB} \cdot z_i^4 + K_{5iB} \cdot z_i^5) \quad (12)$$

where: K_{jiB} are constant coefficients for bending moment (j – exponent, i – number of section), which are calculated as:

$$\begin{cases} K_{1iB} = C_{iB}^2 \\ K_{2iB} = 2 \cdot B_{iB} \cdot C_{iB} \\ K_{3iB} = \frac{B_{iB}^2 + 2 \cdot A_{iB} \cdot C_{iB}}{3} \\ K_{4iB} = \frac{A_{iB} \cdot B_{iB}}{2} \\ K_{5iB} = \frac{A_{iB}^2}{5} \end{cases} \quad (13)$$

where: A_{iB} , B_{iB} , C_{iB} are constant coefficients, calculated with Eq. (3).

According Eq. (11) and Eq. (12) and Fig. 5, strain energy from the work of bending moments equals as sum of $(U_B)_i$:

$$U_B = \sum_{i=1}^4 (U_B)_i = \frac{q^2}{E \cdot I_X} \cdot \sum_{i=1}^4 (K_{1iB} \cdot z_i + K_{2iB} \cdot z_i^2 + K_{3iB} \cdot z_i^3 + K_{4iB} \cdot z_i^4 + K_{5iB} \cdot z_i^5) = K_{U_B} \cdot \frac{q^2}{E \cdot I_X} \quad (14)$$

where: K_{U_B} is a constant coefficient.

Strain energy for the i -th section from the work of torque accounts to Eq. (4), Eq. (5) and Eq. (11) because of the symmetry can be calculated as:

$$(U_T)_i = \frac{1}{2} \int_l \frac{2 \cdot M_{iT}^2}{G \cdot I_T} dz = q^2 \Delta^2 \cdot \int_l \frac{(B_{iT} \cdot z + C_{iT})^2}{G \cdot I_T} dz$$

Or in more convenient form as:

$$(U_T)_i = \frac{q^2 \Delta^2}{G \cdot I_T} \cdot (K_{1iT} \cdot z_i + K_{2iT} \cdot z_i^2 + K_{3iT} \cdot z_i^3) \quad (15)$$

where: K_{jiT} are constant coefficients for torque (j – exponent, i – number of section), which are calculated as:

$$\begin{cases} K_{1iT} = C_{iT}^2 \\ K_{2iT} = 2 \cdot B_{iT} \cdot C_{iT} \\ K_{3iT} = \frac{B_{iT}^2}{3} \end{cases} \quad (16)$$

where: B_{iT} , C_{iT} are constant coefficients, calculated with Eq. (6).

According Eq. (11) and Eq. (15) and Fig. 5, strain energy from the work of torque equals as sum of $(U_T)_i$:

$$U_T = \sum_{i=1}^4 (U_T)_i = \frac{q^2 \Delta^2}{G \cdot I_T} \cdot \sum_{i=1}^4 (K_{1iT} \cdot z_i + K_{2iT} \cdot z_i^2 + K_{3iT} \cdot z_i^3) = K_{U_T} \cdot \frac{q^2}{G \cdot I_T} \quad (17)$$

where: K_{U_T} is a constant coefficient.

The coefficients K_{U_B} and K_{U_T} are calculated with account of the data of Tab. 1 and Tab. 2.

Tab. 3 presents the values of K_{U_B} , U_B , K_{U_T} and U_T obtained using Eq. (14) and Eq. (17) for different pallet sizes.

Tab. 3. The values of coefficients K_{U_B} and K_{U_T} and expressions for calculating the values of strain energy from the works of bending moments and torque

Type of pallet	K_{U_B} , m ⁵	U_B , J	K_{U_T} , m ⁵	U_T , J
Euro pallet	$3 \cdot 10^{-4}$	$\frac{3 \cdot 10^{-4} q^2}{E \cdot I_X}$	$4.7 \cdot 10^{-6}$	$\frac{4.7 \cdot 10^{-6} q^2}{G \cdot I_T}$
Industrial pallet	$3.3 \cdot 10^{-4}$	$\frac{3.3 \cdot 10^{-4} q}{E \cdot I_X}$	$3.2 \cdot 10^{-6}$	$\frac{3.2 \cdot 10^{-6} q^2}{G \cdot I_T}$

According to Eq. (11), Eq. (14) and Eq. (17), the strain energy of the stopper equals as:

$$U = q^2 \cdot \left(\frac{K_{U_B}}{E \cdot I_X} + \frac{K_{U_T}}{G \cdot I_T} \right)$$

Therefore, allowable strain energy of the stopper is found as:

$$[U] = [q]^2 \cdot \left(\frac{K_{U_B}}{E \cdot I_X} + \frac{K_{U_T}}{G \cdot I_T} \right)$$

where: $[q]$ is allowable distributed load.

Taking into account Eq. (10), $[U]$ is calculated as:

$$[U] = [\sigma]^2 \cdot \frac{\left(\frac{K_{U_B}}{E \cdot I_X} + \frac{K_{U_T}}{G \cdot I_T} \right)}{\left(\frac{K_B \cdot Y_{MAX}}{I_X} \right)^2 + 3 \left(\frac{K_T \cdot R_{MAX}}{I_T} \right)^2} \quad (18)$$

4. ALLOWABLE PALLET SPEED

Assuming the pallet as an absolutely rigid body, the kinetic energy of the pallet during the impact is converted into the strain energy of the stopper. Weight of the pallet with the load is at least an order of magnitude greater than the mass of the stopper. Therefore, the Cox impact theory can be used in engineering calculations (Ol'shanskii V.P. and Ol'shanskii S.V., 2013), and the allowable speed of a pallet is determined by the allowable strain energy of the stopper.

Taking into account the smallness of the angle of inclination of the gravity roller conveyor in pallet flow rack (no more than 2–3 degrees), the impact can be regarded as longitudinal with a sufficient degree of accuracy. Therefore, the kinetic energy of the pallet is equal to the strain energy of the stopper:

$$\frac{M \cdot [v]^2}{2} = [U] \quad (19)$$

where: M – weight of the pallet, $[v]$ – allowable speed of the pallet.

According to Eq. (18) and Eq. (19), the allowable speed for pallets in the pallet flow rack is calculated as:

$$[v] = [\sigma] \sqrt{\frac{2}{M} \cdot \frac{\left(\frac{K_{U,B} + K_{U,T}}{E \cdot I_X} + \frac{K_{U,T}}{G \cdot I_T}\right)}{\left(\frac{K_{B,Y_{MAX}}}{I_X}\right)^2 + 3 \left(\frac{K_{T,R_{MAX}}}{I_T}\right)^2}} \quad (20)$$

5. CALCULATION EXAMPLE

For the stopper shown in Fig. 6, made of a tube 40 x 40 x 3.5 and welded to it along the entire length of the steel plate 6 mm thick, we have the following data:

$$E = 2.1 \cdot 10^{11} \text{ Pa}; G = 8.2 \cdot 10^{10} \text{ Pa}; [\sigma] = 2.2 \cdot 10^8 \text{ Pa}$$

$$I_X = 3.02 \cdot 10^{-7} \text{ m}^4; I_X = 3.0 \cdot 10^{-7} \text{ m}^4; I_T = 1.54 \cdot 10^{-7} \text{ m}^4$$

$$y_{MAX} = 26 \cdot 10^{-3} \text{ m}; R_{MAX} = 20 \cdot 10^{-3} \text{ m}$$

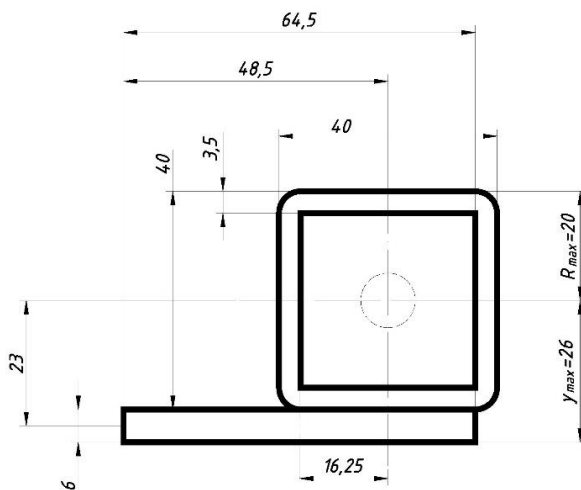


Fig. 6. Example of the stopper construction (cross-section view)

Fig. 7 presents the dependence of the allowable speed for pallets on its type and mass for the construction described above and calculated with Eq. (16).

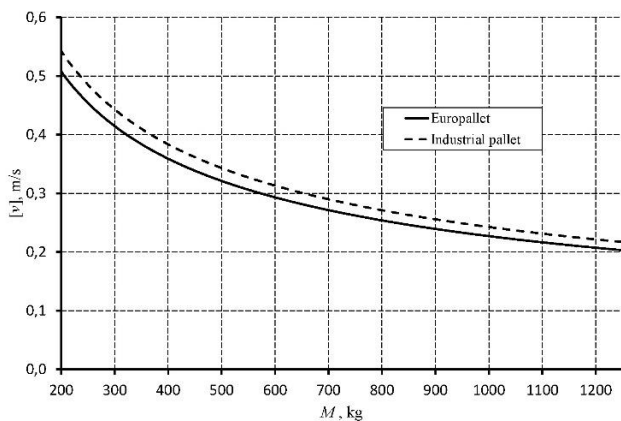


Fig. 7. Dependence of the allowable speed for pallets on its type and mass

6. CONCLUSION

1. The calculation method, based on the Cox impact theory, was developed to calculate the allowable speed for the pallets of different masses in a pallet flow rack.
2. The method takes into account the type of pallet, construction and material of the stopper.
3. Calculation examples of the allowable speed for the Euro pallet and Industrial pallet are presented for the stopper, made from square cross-section tube 40 x 40 x 3.5 mm with the welded plate of 6 mm thickness.
4. The calculated results agree well with the speed range of 0.2 to 0.3 m/s recommended by the manufacturers.

REFERENCES

1. Accorsi, R., Baruffaldi, G., Manzini, R. (2017), Design and manage deep lane storage system layout. An iterative decision-support model, *Int J Adv Manuf Technol*, 92(1-4), 57–67.
2. Aleksandrov A.A., Devisilov V.A., Ivanov M.V. (2016), A role of education system in creation of safety culture, *Chemical Engineering Transactions*, 53, 211–216.
3. Boysen, N., Boywitz, D., Weidinger, F. (2018), Deep-lane storage of time-critical items: one-sided versus two-sided access, *OR Spectrum*, 40(4), 1141–1170.
4. Boywitz, D., Boysen, N. (2018), Robust storage assignment in stack- and queue-based storage systems, *Computers & Operations Research*, 100, 189–200.
5. Crisan, A., Ungureanu, V., Dubina, D. (2012), Behaviour of cold-formed steel perforated sections in compression. Part 1-Experimental investigations, *Thin-walled structures*, 61, 86–96.
6. Derhami, S., Smith, JS., Gue, KR. (2017), Optimising space utilisation in block stacking warehouses, *Int J Of Prod Res*, 55(21), 6436–6452.
7. *Dynamic storage catalogue Damon* [available at: <http://damon-group.com.au/catalogues/dynamic-storage-catalogue.pdf>, access 29 March 2017].
8. Eo, J., Sonico, J., Su, A., Wang, W., Zhou, C., Zhu, Y., Wu, S., Chokshi, T. (2015), Structured comparison of pallet racks and gravity flow racks, *IIE Annual Conference and Expo 2015*, 1971–1980.
9. *EPAL Euro Pallet* [available at <https://www.epal-pallets.org/en/load-carriers/epal-euro-pallet>, access 7 December, 2017]
10. *Gesamtkatalog_2012_D.pdf* [available at: http://www.euroroll.de/tl_files/Gesamtkatalog_2012_D.pdf, access 29 March 2017].
11. Ghalekhondabi, I., Masel, DT. (2018), Storage allocation in a warehouse based on the forklifts fleet availability, *Journal Of Algorithms & Computational Technology*, 12(2), 127–135.
12. Ghomri, L., Sari, Z. (2017), Mathematical modeling of the average retrieval time for flow-rack automated storage and retrieval systems, *Journal Of Manufacturing Systems*, 44, 165–178.
13. Halim, N.H.A., Jaffar, A., Yusoff, N., Adnan, A.N. (2012), Gravity Flow Rack's material handling system for Just-in-Time (JIT) production, *2nd International Symposium on Robotics and Intelligent Sensors 2012, IRIS 2012, Procedia Engineering*, 41, 1714–1720.
14. Hamzaoui, MA., Sari, Z. (2015), Optimal dimensions minimizing expected travel time of a single machine flow rack AS/RS, *Mechatronics*, 31, 158–168.
15. Heragu, SS., Cai, X., Krishnamurthy, A., Malmborg, CJ. (2011), Analytical models for analysis of automated warehouse material handling systems, *Int J Of Prod Res*, 49(22), 6833–6861.
16. *Interroll Pallet Roller Flow PF 1100* [available at: https://www.interroll.ru/fileadmin/products/en/Resources_pdf_344683531.pdf, access 29 March 2017].

17. **Jones R.** (2009), *Deformation theory of plasticity*, Bull Ridge Publishing, USA.
18. **Kulwiec R.** (1985), *Material handling handbook*, 2nd edition, John Wiley & Sons, Inc, USA.
19. **Lerher, T., Borovinsek, M., Ficko, M., Palcic, I.** (2017), Parametric study of throughput performance in SBs/Rs based on simulation, *Int J Of Simul Model*, Vol. 16, No. 1, 96–107.
20. *Live pallet racking* [available at: https://mecaluxuk.cdnwm.com/catalogues/live-pallet-racking3.1.0.pdf#_ga=1.79741783.1709563512.1490605253, access 29 March 2017].
21. **Metahri, D., Hachemi, K.** (2017), Automated storage and retrieval systems: a performances comparison between Free-fall-flow-rack and classic flow-rack, *6-th International Conference On Systems And Control (ICSC' 17)*, Edited by: Drid, S., Mehdi D., Aitouche, A., 589–594.
22. **Nash W.** (1998), *Schaum's Outline of Theory and Problems of Strength of Materials*, 4-th edition, McGraw-Hill, USA.
23. **Nosko A.L., Safronov E.V., Soloviev V.A.** (2018), Study of Friction and Wear Characteristics of the Friction Pair of Centrifugal Brake Rollers, *Journal of Friction and Wear*, 39(2), 145–151.
24. **Ol'shanskii V.P., Ol'shanskii S.V.** (2013), Calculation of the dynamic deflection of a beam on inelastic impact by the Cox and Saint-Venant theories, *Strength of materials*, 45(3), 361–368.
25. *POT R M-029-2003 (2003)*, Mezhotraslevyye pravila po okhrane truda pri ekspluatatsii promyshlennogo transporta (konveyernyy, truboprovodnyy i drugiye transportnyesredstva nepreryvnogo deystviya, Izd-vo NTS ENAS, Moscow (in Russian).
26. *Rollenbahnen-Trennvorrichtung* [available at: http://www.rackandroll.de/default.aspx?Pagename=Rollenbahnen_Trennvorrichtung, access 29 March 2017] (in Deutsch).
27. **Rushton A., Croucher P., Baker P.** (2010), *The handbook of logistics & distribution management*, 4th edition, Kogan Page Limited, London.
28. **Saleh, A., Far, H., Mok, L.** (2018), Effects of different support conditions on experimental bending strength of thin walled cold formed steel storage upright frames, *Journal of constructional steel research*, 150, 1–6.
29. **Sulirova, I., Zavodska, L., Rakyta, M., Pelantova, V.** (2017), State-of-the-art approaches to material transportation, handling and warehousing, *12th International scientific conference of young scientists on sustainable, modern and safe transport, Procedia Engineering*, 192, 857–862.
30. **Talebian, N., Gilbert, BP., Pham, CH, Chariere, R., Karampour, H.** (2018), Local and Distortional Biaxial Bending Capacities of Cold-Formed Steel Storage Rack Uprights, Proceedings of the 7th International Conference on Coupled Instabilities in Metal Structures, *Journal of Structural Engineering*, 144, No. 6.
31. **Thombare C.N., Sangle K.K., Mohitkar V.M.** (2016), Nonlinear buckling analysis of 2-D cold-formed steel simple cross-aisle storage rack frames, *Journal of Building Engineering*, 7, 12–22.
32. **Vujanac R., Miloradovic N., Vulovic S.** (2016), Dynamic storage systems, *ANNALS of Faculty Engineering Hunedoara – International Journal of Engineering*, XIV, 79–82.
33. **Wu S., Wu Ya., Wang Ya.** (2016), A structured comparison study on storage racks system, *Journal of Residuals Science & Technology*, 13(8), 2016.
34. **Zaerpour, N., Yu, YG., de Koster RBM** (2015), Storing Fresh Produce for Fast Retrieval in an Automated Compact Cross-Dock System, *Production And Operations Management*, 24(8), 1266–1284.